

Impact of Ba Substitution on the Magnetocaloric Effect in $\text{La}_{1-x}\text{Ba}_x\text{MnO}_3$ Manganites

Imad Hussain, M. S. Anwar, Eunji Kim, Bon Heun Koo, and Chan Gyu Lee[†]

School of Materials Science and Engineering, Changwon National University, Changwon 51140, Republic of Korea

(Received June 29, 2016 : Revised October 10, 2016 : Accepted October 10, 2016)

Abstract $\text{La}_{1-x}\text{Ba}_x\text{MnO}_3$ ($x = 0.30, 0.35$ and 0.40) samples have been prepared by solid-state reaction method. The X-ray diffraction (XRD) study showed that all the samples crystallized in a rhombohedral structure with an R-3c space group. Variation of the magnetization as a function of the temperature and applied magnetic field was carried out. All the samples revealed ferromagnetic to paramagnetic (FM-PM) phase transition at the Curie temperature $T_C \sim 342$ K. The magnetic entropy change was also studied through examination of the measured magnetic isotherms $M(H, T)$ near T_C . The magnetocaloric effect was calculated in terms of the isothermal magnetic entropy change. The maximum entropy change reaches a value of 1.192 J/kgK under a magnetic field change of 2.5 T for the $\text{La}_{0.6}\text{Ba}_{0.4}\text{MnO}_3$ composition. The relative cooling power (RCP) is 79.31 J/kg for the same applied magnetic field.

Key words magnetocaloric effect, magnetization, magnetic entropy, relative cooling power.

1. Introduction

Magnetic refrigeration is a very promising alternative to conventional gas compression refrigeration regarding to energy savings and environmental considerations.¹⁻³⁾ Magnetic refrigeration is based on the magnetocaloric effect which is an intrinsic thermodynamic property of a magnetic material. The magnetocaloric effect (MCE) refers to the temperature change for a magnetic material under the application of an adiabatically applied external magnetic field. The externally applied magnetic field causes the spins to be aligned in a ferromagnetic material. This alignment of spins with the applied magnetic field results in a decrease in the magnetic entropy and an increase in the lattice entropy thereby increasing the temperature of the material. After removing the field, the spins rearrange randomly, the magnetic entropy increases which causes a reduction in the lattice entropy and hence the temperature is decreased.^{4,5)} In general there are three key requirements for a magnetic material to be considered as a potential magnetic refrigerant: the maximum in magnetic entropy change, adiabatic temperature change and the relative cooling power.^{6,7)} Among them, the relative cooling power is the most meaningful parameter which

provides a measure of the effectiveness of a material to be used for magnetic refrigeration. Mixed valence perovskites based on manganese oxides with general formula $\text{A}_{1-x}\text{B}_x\text{MnO}_3$ (where A is a trivalent cation like La, Nd or Pr, and B is a divalent cation like Ca, Sr, Pb) have been studied extensively for their high transport and magnetic properties and also for the features of technological interest like colossal magnetoresistance, unconventional insulator-metal transitions and magnetocaloric effect.⁸⁻¹¹⁾ The complex electronic behavior of mixed valence perovskites is largely governed by the double exchange interaction. This double exchange interaction is triggered by the conversion of Mn^{3+} into Mn^{4+} by doping the divalent type B ions into the original AMnO_3 compound. At present, besides some possible candidates, such as $\text{Gd}_5(\text{Si}_{1-x}\text{Ge}_x)_4$,¹²⁾ $\text{MnAs}_{1-x}\text{Sb}_x$,¹³⁾ $\text{MnFeP}_{1-x}\text{As}_x$,¹⁴⁾ and $\text{Tb}_{1-x}\text{Gd}_x\text{Al}_2$,¹⁵⁾ the hole-doped manganites can be used as potential magnetic refrigerants for cooling applications over a wide range of operating temperature.¹⁶⁾ In particular, LaSr-, LaCa- and LaBa-based manganites have been studied extensively because of the possibility for producing room temperature magnetic refrigeration technology based on their low cost of production, chemical stability and easy tailoring of magnetic properties.¹⁶⁾ In

[†]Corresponding author

E-Mail : chglee@changwon.ac.kr (C. G. Lee, Changwon Nat'l Univ.)

© Materials Research Society of Korea, All rights reserved.

This is an Open-Access article distributed under the terms of the Creative Commons Attribution Non-Commercial License (<http://creativecommons.org/licenses/by-nc/3.0>) which permits unrestricted non-commercial use, distribution, and reproduction in any medium, provided the original work is properly cited.

the present work, we investigated the effect of different doping content of Ba on the magnetic and magnetocaloric properties of $\text{La}_{1-x}\text{Ba}_x\text{MnO}_3$.

2. Experimental Procedure

The $\text{La}_{1-x}\text{Ba}_x\text{MnO}_3$ ($x = 0.30, 0.35, 0.40$) samples were synthesized by means of conventional solid state reaction method. Stoichiometric amounts of highly pure (99.99 %) La_2O_3 , BaO , and Mn_2O_3 precursor powders were mixed thoroughly in ethanol and were put for ball milling for 10 hours. The mixture powders were dried for 10 h at 90°C and then heated in alumina crucibles at 1000°C in air for 12 h. The resulting powders were grind and then pressed into pellets with a diameter of 7 mm and a thickness of about 1 mm. The pellets were first sintered at 1100°C for 48 h followed by repeated grinding. After final sintering performed at 1300°C for 24 h in air, all the samples were cooled to room temperature at a cooling rate of $5^\circ\text{C}/\text{min}$.

The crystal structure, homogeneity and the phase purity were determined at room temperature by means of X-ray powder diffraction (XRD) using $\text{Cu K}\alpha$ radiation (Bruker D8 Advance). The microstructure of each sample was investigated by using scanning electron microscope (SEM, JSM5610). The magnetization measurements were performed in the temperature range of 100–380 K at a frequency of 40 Hz by using a quantum design vibrating

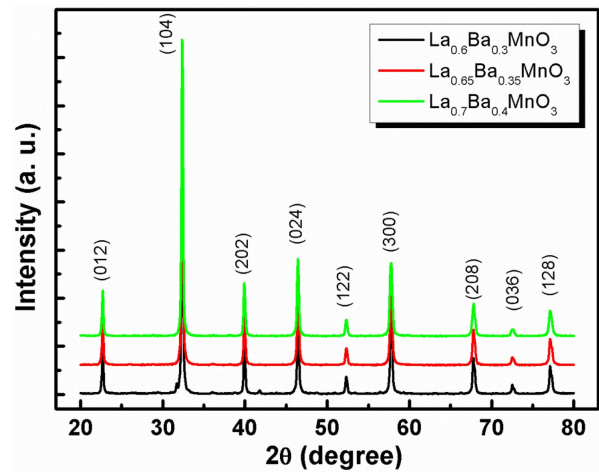


Fig. 1. Room temperature XRD patterns of $\text{La}_{1-x}\text{Ba}_x\text{MnO}_3$ ($x = 0.30, 0.35, 0.40$) samples.

sample magnetometer (PPMS-6000). In order to evaluate the magnetic entropy, the magnetization isotherms were recorded at small temperature intervals around T_C in magnetic fields up to 2.5 T.

3. Results and Discussion

Fig. 1 shows the XRD patterns of the $\text{La}_{1-x}\text{Ba}_x\text{MnO}_3$ ($x = 0.30, 0.35, 0.40$) (LBMO) samples. The XRD patterns for LBMO samples indicate the formation of a single

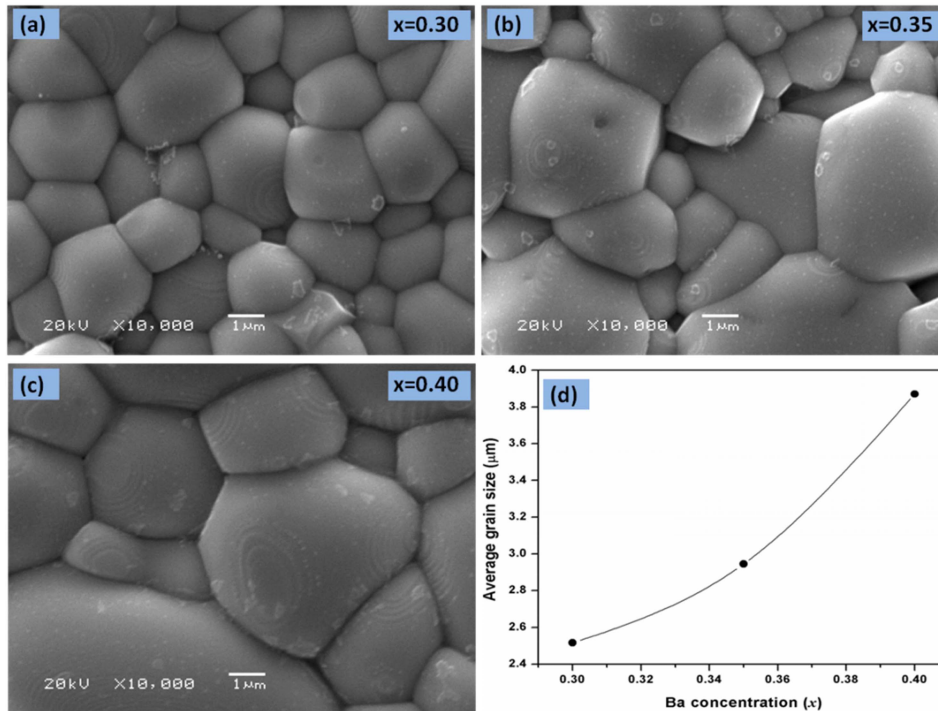


Fig. 2. Scanning electron micrographs of $\text{La}_{1-x}\text{Ba}_x\text{MnO}_3$ samples sintered at 1300°C . (a) $x = 0.30$, (b) $x = 0.35$, (c) $x = 0.40$, (d) The variation in average grain size as a function of Ba concentration.

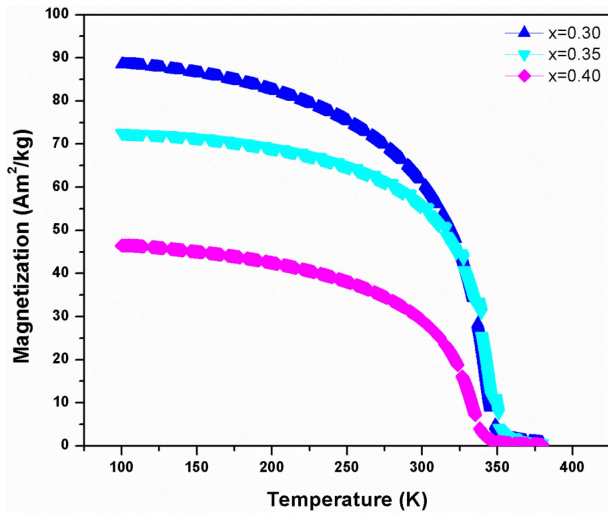


Fig. 3. Temperature dependence of magnetization for $\text{La}_{1-x}\text{Ba}_x\text{MnO}_3$ ($x = 0.30, 0.35, 0.40$) samples measured at an applied field of 0.1 T.

phase without a detectable impurity peak. The peaks in the XRD patterns can be indexed in the rhombohedral system with R-3C space group for all synthesized samples according to ICDD file 01-072-8053. From the XRD pattern, LBMO clearly exhibits a polycrystalline behavior with maximum intensity for the (104) reflection. Figs. 2(a,b) and (c) show the scanning electron microscopy (SEM) results for all synthesized LBMO samples with same magnification. All the compositions are homogeneous with strongly connected grains. The variation of the average grain size with the increasing Ba doping is shown in Fig. 2(d). The average grain size was estimated by using ImageJ software and was found to be $\sim 2.51, 2.94$ and $3.87 \mu\text{m}$ for $x = 0.30, 0.35$ and 0.40 composition respectively. The increase in the average grain size with the increasing Ba doping indicates that the incorporation of Ba into La-sites promotes the grain growth during sintering process at 1300°C . The temperature dependent

magnetization $M(T)$ curves measured under an applied magnetic field of 0.1 T for LBMO samples are shown in Fig. 3. It can be seen in Fig. 3 that the magnetization decreases with the increasing Ba doping, further maximum saturation magnetization is just below $90 \text{ Am}^2/\text{kg}$ for $\text{La}_{0.7}\text{Ba}_{0.3}\text{MnO}_3$ sample at 100 K. The M-T data plots show that all samples undergo a paramagnetic to ferromagnetic (PM-FM) phase transition upon cooling and the magnetization for each sample drops rapidly at the Curie temperature. The rapid drop in magnetization with respect to the temperature suggests a large MCE in the vicinity of the Curie temperature. The Curie temperature T_C , defined by the minimum of the derivative of magnetization with respect to temperature (dM/dT) in the M-T curve, has been determined to be 342 K for $\text{La}_{0.7}\text{Ba}_{0.3}\text{MnO}_3$ and 333 K for $\text{La}_{0.6}\text{Ba}_{0.4}\text{MnO}_3$, suggesting that T_C decreases with increasing Ba substitution.

Fig. 4 shows isothermal magnetization curves at different temperatures for the $\text{La}_{0.7}\text{Ba}_{0.3}\text{MnO}_3$ and $\text{La}_{0.6}\text{Ba}_{0.4}\text{MnO}_3$ samples in the magnetic field range of 0-2.5 T. For both samples, a dramatic change in the magnitude of magnetization can be observed around T_C . At temperatures below T_C , the magnetization increases sharply even at low field values and tends to saturate as the field increases. In order to obtain a deeper insight into the type of magnetic phase transition, Banerjee criterion was used.¹⁷⁾ Arrott plots (H/M vs. M^2) were obtained from isothermal magnetization data and the results are plotted in Fig. 5. According to Banerjee's criterion the slope of the Arrott plots stipulates whether the observed magnetic phase transition is of first order (negative slope) or second order (positive slope). For both samples, a second order magnetic phase transition can be clearly observed due to positive slope in the high temperature regions. Based on a series of isothermal magnetization curves, one can calculate the magnetic entropy changes ΔS_M by using the following Maxwell equation^{18,19)}:

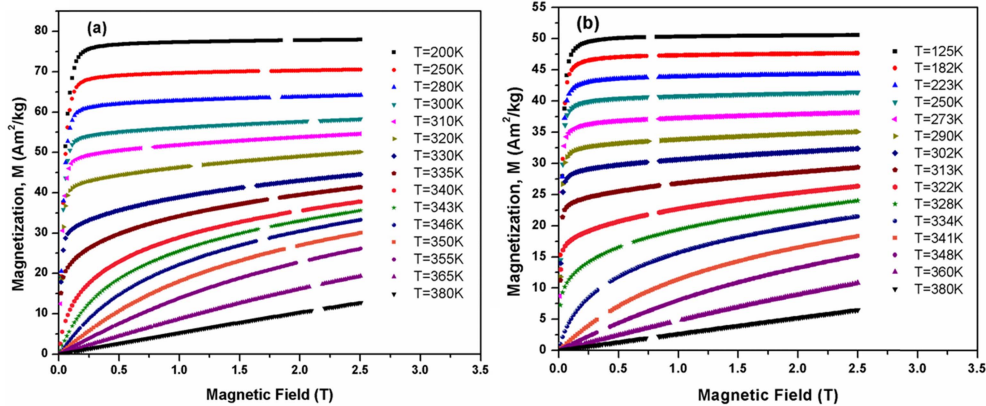


Fig. 4. The field dependence of magnetization for $\text{La}_{1-x}\text{Ba}_x\text{MnO}_3$ samples measured at different temperatures around T_C (a) $x = 0.30$, (b) $x = 0.40$.

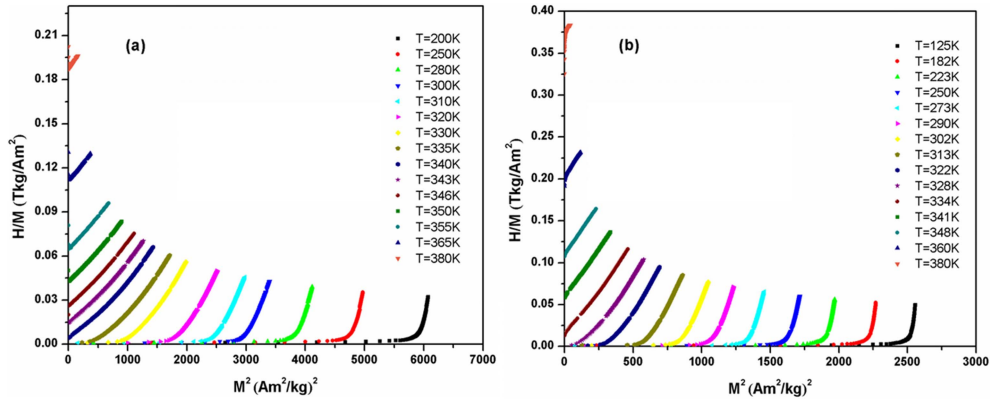


Fig. 5. Arrott plots (H/M vs. M^2) for $\text{La}_{1-x}\text{Ba}_x\text{MnO}_3$ samples (a) $x = 0.30$, (b) $x = 0.40$.

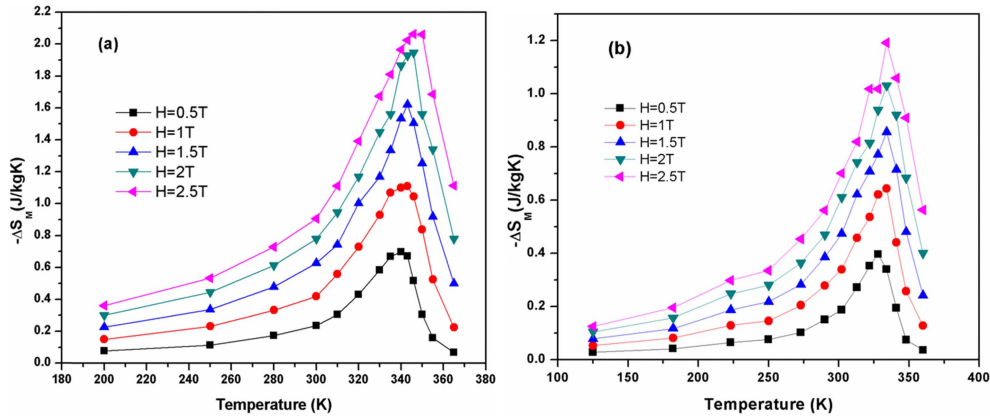


Fig. 6. Temperature dependence of magnetic entropy change measured at different applied magnetic fields for $\text{La}_{1-x}\text{Ba}_x\text{MnO}_3$ samples (a) $x = 0.30$, (b) $x = 0.40$.

$$\Delta S_M(T, H) = S_M(T, H) - S_M(T, 0) = \int_0^H \left(\frac{\partial M(T, H)}{\partial T} \right)_H dH \quad (1)$$

Where M represents the magnetization, H is the applied magnetic field and T is the temperature. From Eq. (1) it is clear that the magnetic entropy change ΔS_M depends on the temperature gradient of the magnetization and achieves a maximum value near the Curie temperature. In practice for magnetization measurement at small discrete field and temperature intervals, the magnetic entropy change ΔS_M can be approximated by

$$|\Delta S_M| = \sum_i \frac{M_i - M_{i+1}}{T_{i+1} - T_i} \Delta H_i \quad (2)$$

Where M_i and M_{i+1} are the experimental values of the magnetization measured in a magnetic field H_i at temperatures T_i and T_{i+1} respectively. A strong variation in magnetization can be observed in the M - H curves around T_C which suggests a possible large magnetic entropy change associated with the FM-PM transition. With the decrease in temperature, the value of magnetization has been found to increase in the temperature range of 125 to

380 K, where the thermal fluctuation of spins decreases with decreasing temperature.

From isothermal magnetization curves M - H , we calculated the magnetic entropy changes $\Delta S_M(T, H)$ by using Eq. (2). The magnetic entropy change $[-\Delta S_M(T, H)]$ for $\text{La}_{0.7}\text{Ba}_{0.3}\text{MnO}_3$ and $\text{La}_{0.6}\text{Ba}_{0.4}\text{MnO}_3$ composition as a function of temperature in the magnetic field range of 0.5 to 2.5 T is shown in Fig. 6. All the curves reveal that the maximum value of the magnetic entropy change ($-\Delta S_M^{\max}$) increases with the increase in applied magnetic field, keeping the peak position nearly unaffected. The peak in the entropy change curves can be found close to the Curie temperature where the variation of magnetization with temperature is maximum. The maximum value of the ($-\Delta S_M^{\max}$) is found to be 2.06 J/kgK for $\text{La}_{0.7}\text{Ba}_{0.3}\text{MnO}_3$ sample at an applied magnetic field of 2.5 T. The increase in the value of the ($-\Delta S_M^{\max}$) with the increasing applied magnetic field indicates a much larger magnetic entropy change to be expected at higher magnetic field.

The relative cooling power(RCP) is the most meaningful parameter which is used to evaluate the cooling efficiency

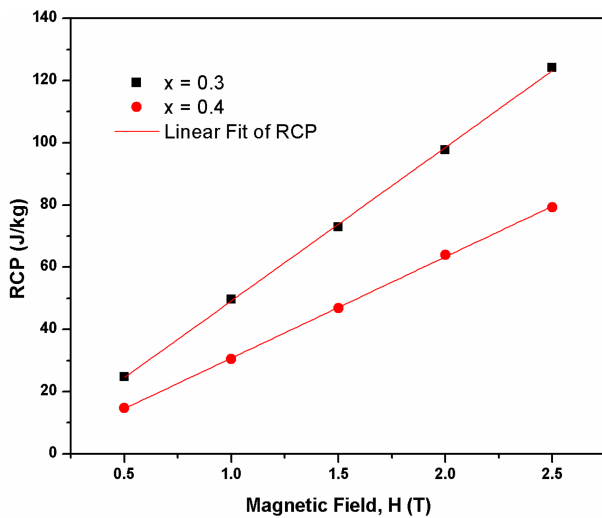


Fig. 7. The relative cooling power (RCP) values vs. applied magnetic field for $\text{La}_{1-x}\text{Ba}_x\text{MnO}_3$ samples (a) $x = 0.30$, (b) $x = 0.40$.

of a magnetic material for applications in magnetic refrigeration. A material with a high RCP value is considered as a good material for magnetic refrigeration. The RCP corresponds to the amount of heat transferred between the hot and cold parts of the refrigerator in an ideal thermodynamic cycle.^{16,20} Mathematically, the RCP is defined as

$$RCP = -\Delta S_M(T, H) \delta T_{FWHM} \quad (3)$$

Where δT_{FWHM} is the full width at half maximum of the magnetic entropy change curve. Fig. 7 shows the RCP values plotted against the applied magnetic field for $\text{La}_{0.7}\text{Ba}_{0.3}\text{MnO}_3$ and $\text{La}_{0.6}\text{Ba}_{0.4}\text{MnO}_3$ samples. A nearly linear variation in the RCP values with the applied magnetic field is observed. It can be seen from Fig. 7 that the value of RCP increases with the increasing magnetic field and reaches the value of 124 J/kg at an applied magnetic field of 2.5 T for $\text{La}_{0.7}\text{Ba}_{0.3}\text{MnO}_3$ composition. This high value of RCP suggests that this sample can be used as potential magnetic refrigerant with a wide range of operating temperature.

4. Conclusions

We have investigated the magnetic and magnetocaloric properties of $\text{La}_{1-x}\text{Ba}_x\text{MnO}_3$ ($x = 0.30, 0.35, 0.40$) polycrystalline samples. The X-ray powder diffraction measurements show that all the samples crystallize in rhombohedral structure. The magnetization versus temperature curves showed a ferromagnetic to paramagnetic transition for all the synthesized samples. A considerable reduction in the value of saturation magnetization was observed

with the increasing Ba doping. The magnetic entropy change was investigated from the isothermal magnetization versus magnetic field data measured at different temperatures. It was found that the maximum magnetic entropy change increases with the increasing magnetic field. The relatively large value of ΔS_M (1.192 J/kgK) and RCP (79.31 J/kg) shows that $\text{La}_{0.6}\text{Ba}_{0.4}\text{MnO}_3$ sample can be considered as an active magnetic refrigerant near room temperature.

Acknowledgment

This research is financially supported by Changwon National University in 2015~2016.

References

1. K. A. Gschneidner Jr, V. K. Pecharsky and A. O. Tsokol, Rep. Prog. Phys., **68**, 1479 (2005).
2. M. S. Anwar and B. H. Koo, Eelectron. Mater. Lett., **11**, 614 (2015).
3. I. Hussain, M. S. Anwar, J. W. Kim, K. C. Chung and B. H. Koo, Ceram. Int., **42**, 13098 (2016).
4. B. F. Yu, Q. Guo, B. Zhang, X. Z. Meng and Z. Chen, Int. J. Refrig., **26**, 622 (2003).
5. M. H. Phan and S. C. Yu, J. Magn. Magn. Mater., **308**, 325 (2007).
6. R. Caballero-Flores, V. Franco, A. Conde, K. E. Knippling and M. A. Willard, Appl. Phys. Lett., **98**, 102501 (2011).
7. K. A. Gschneidner Jr and V. K. Pecharsky, Annu. Rev. Mater. Sci., **30**, 387 (2000).
8. Y. Tokura, Rep. Prog. Phys., **69**, 797 (2006).
9. J. B. Goodenough, Rep. Prog. Phys., **67**, 1915 (2004).
10. J. Paul Attfield, Chem. Mater., **10**, 3239 (1998).
11. A. J. Millis, Nature, **392**, 147 (1998).
12. V. K. Pecharsky and K. A. Gschneidner Jr, Phys. Rev. Lett., **78**, 4494 (1997).
13. H. Wada and Y. Tanabe, Appl. Phys. Lett., **79**, 3302 (2001).
14. Q. Tegu, E. Bruck, K.H. Buschow and F. R. de Boer, Nature, **415**, 150 (2002).
15. F. W. Wang, X. X. Zhang and F. X. Hu, Appl. Phys. Lett., **77**, 1360 (2000).
16. M. H. Phan and S. C. Yu, J. Magn. Magn. Mater., **308**, 325 (2007).
17. B. K. Banerjee, Phys. Lett., **12**, 16 (1964).
18. I. Hussain, M. S. Anwar, S. R. Lee and B. H. Koo, J. Supercond. Nov. Magn., **28**, 3323 (2015).
19. Z. M. Wang, G. Ni, Q. Y. Xu, H. Sang and Y. M. Du, J. Appl. Phys., **90**, 5689 (2001).
20. A. Rostamnejadi, M. Venkatesan, P. Kameli, H. Salamati and J. M. D. Coey, J. Magn. Magn. Mater., **323**, 2214 (2011).